Monthly Notices of the ROYAL ASTRONOMICAL SOCIETY
MNRAS **503,** 1214–1220 (2021) doi:10.1093/mnras/stab349

High-frequency radio observations of two magnetars, PSR J1622 − 4950 and 1E 1547.0 − 5408

Che-Yen Chu,[1]★ C.-Y. Ng,[2] Albert K. H. Kong [1] and Hsiang-Kuang Chang [1]
[1]*Institute of Astronomy, National Tsing Hua University, Hisnchu City 300044, Taiwan*
[2]*Department of Physics, The University of Hong Kong, Pokfulam Road, Hong Kong, China*

Accepted 2021 January 29. Received 2021 January 29; in original form 2020 May 27

ABSTRACT

We investigated the radio spectra of two magnetars, PSR J1622 − 4950 and 1E 1547.0 − 5408, using observations from the Australia Telescope Compact Array and the Atacama Large Millimeter/submillimeter Array obtained in 2017. Our observations of PSR J1622 − 4950 show a steep spectrum with a spectral index of -1.3 ± 0.2 in the range of 5.5–45 GHz during its reactivating X-ray outburst in 2017. By comparing the data taken in different epochs, we found a significant enhancement in the radio flux density. The spectrum of 1E 1547.0 − 5408 was inverted in the range of 43–95 GHz, suggesting a spectral peak at a few hundred gigahertz. Moreover, we obtained X-ray and radio data of the radio magnetars PSR J1622 − 4950 and SGR J1745 − 2900 from the literature and found two interesting properties. First, radio emission is known to be associated with X-ray outbursts but has a different evolution; furthermore, we found that the rise time of the radio emission is much longer than that of the X-ray emission during the outburst. Second, radio magnetars may have double-peak spectra at a few GHz and a few hundred GHz. This could indicate that the emission mechanism is different in the cm and the submm bands. These two phenomena could provide a hint towards an understanding of the origin of radio emission and its connection with X-ray properties.

Key words: stars: magnetars – stars: neutron – pulsars: individual: PSR J1622 − 4950 – pulsars: individual: 1E 1547.0 − 5408 – radio continuum: stars.

1 INTRODUCTION

Magnetars are isolated neutron stars with strong magnetic fields $\gtrsim 10^{14}$ G (Duncan & Thompson 1992). Unlike the case for rotation-powered pulsars, the X-ray luminosities of magnetars are not caused solely by rotational energy loss. Instead, their strong magnetic fields provide the energy to power the observed X-ray emission. Magnetars manifest themselves as soft gamma repeaters (SGRs) or anomalous X-ray pulsars (AXPs) in observations. SGRs and AXPs were first discovered in the X-ray as neutron stars with slow rotation periods (1–12 s) showing burst activity. Currently, there are 24 confirmed magnetars (Olausen & Kaspi 2014),[1] and only five of them show pulsed radio emission, in which the radio spectra are either flat or inverted (Camilo et al. 2006, 2007a; Levin et al. 2010; Eatough et al. 2013; Shannon & Johnston 2013; Karuppusamy et al. 2020).

An X-ray outburst of a magnetar involves a sudden increase in X-ray flux, sometimes accompanied by multiple short X-ray bursts on millisecond to second time-scales. Sudden magnetar crustal activities can twist the magnetosphere, resulting in an X-ray outburst as observed (Thompson 2008; Beloborodov 2009). The magnetosphere gradually becomes untwisted, so the X-ray flux decreases. The flux of an outburst usually decays on multiple time-scales, with one rapid decay within hours to a day followed by a slow decay of several months to years (e.g. Woods et al. 2004). Most outbursts are associated with radiative phenomena, such as changes in pulse profile, pulsed fraction and multiwavelength emission, and X-ray spectral hardening. Multiwavelength studies of radio-loud magnetars suggest that an X-ray outburst may trigger radio emission (e.g. Halpern et al. 2005; Camilo et al. 2007a; Anderson et al. 2012).

The magnetar 1E 1547.0 − 5408 was discovered in the supernova remnant (SNR) G327.24 − 0.13 (Lamb & Markert 1981) and was later confirmed to be an AXP with a spin period of 2.1 s through X-ray and radio observations (Gelfand & Gaensler 2007; Camilo et al. 2007a). In previous cm observations, 1E 1547.0 − 5408 showed a flat spectrum (Camilo et al. 2008) that is a possible gigahertz-peaked spectrum (GPS; Kijak et al. 2013). The 2007 X-ray observations suggested that there was an X-ray outburst, which could have triggered the radio emission of 1E 1547.0 − 5408 between late 2006 and early 2007 (Halpern et al. 2008). *Swift*/BAT, *Fermi*/GBM and *INTEGRAL*/SPI detected two more outbursts in 2008 October (Israel et al. 2010; Kaneko et al. 2010) and 2009 January (Mereghetti et al. 2009; Savchenko et al. 2010; Kaneko et al. 2010). The 2009 X-ray outburst was more energetic but less variable than the 2008 one (Israel et al. 2010; Ng et al. 2011; Scholz & Kaspi 2011). There was also some short burst activity in 2009 March and 2010 January (Kaneko et al. 2010; von Kienlin et al. 2012; Kuiper et al. 2012). Since 2010, however, there have been no X-ray burst reports for 1E 1547.0 − 5408.

PSR J1622 − 4950 was the first magnetar to be discovered in the radio. At the time of discovery, it showed an inverted spectrum

★ E-mail: cychu@gapp.nthu.edu.tw
[1]McGill Online Magnetar Catalog http://www.physics.mcgill.ca/~pulsar/magnetar/main.html.

from 1.4 to 9.0 GHz with a spectral index of $\alpha = 0.71$ (Levin et al. 2010). The positive index is very rare, as radio pulsars generally have indexes ranging from −2 to −1. In later observations, however, it turned out that the spectrum is not inverted from 17 to 24 GHz (Keith et al. 2011). PSR J1622 − 4950 shows a GPS similar to the spectra of 1E 1547.0 − 5408 observed in 2007 (Kijak et al. 2013). The X-ray data during the epoch of radio discovery of PSR J1622 − 4950 suggest that an X-ray outburst could have happened before 2007 April (Anderson et al. 2012). Follow-up radio observations show that the radio emission decreased to an undetectable level in 2015 (Scholz et al. 2017) until the reactivating X-ray outburst event in 2017 March (Pearlman et al. 2017; Camilo et al. 2018).

Regarding other magnetars with detected radio emission, XTE J1810 − 197 was the first radio-detected magnetar (Camilo et al. 2006) that was discovered after its X-ray outburst (Ibrahim et al. 2004). The radio emission disappeared in 2008 (Camilo et al. 2016) and was then reactivated during the 2018 X-ray outburst (Gotthelf et al. 2019). SGR J1745 − 2900 is a radio magnetar discovered near Sargittarius A∗ in 2013 (Kennea et al. 2013; Mori et al. 2013) and, at 291 GHz, shows the highest-frequency radio detection in a magnetar (Torne et al. 2017). The newly confirmed magnetar Swift J1818.0 − 1607 was discovered on 2020 March 12 with a spin period of 1.36 s (Evans et al. 2020; Enoto et al. 2020; Esposito et al. 2020) and was found to have pulsed radio emission a few days later (Karuppusamy et al. 2020; Esposito et al. 2020). The radio emission of Swift J1818.0 − 1607 was detected in a wide band from 0.65 to 154 GHz. There is another noteworthy magnetar, SGR 1935 + 2154, which was confirmed to be a magnetar in 2014 (Israel et al. 2014). It entered an active state with a forest of short X-ray bursts on 2020 April 27 (Palmer 2020). Later, on April 28, a short radio burst was detected from this object (The CHIME/FRB Collaboration et al. 2020; Bochenek et al. 2020). However, pulsed radio emission was detected at only two epochs (Burgay et al. 2020; Zhu et al. 2020).

There are two rotation-powered pulsars with high magnetic fields ($\sim 4.5 \times 10^{13}$ G), PSR J1846 − 0258 and PSR J1119 − 6127 (Gotthelf et al. 2000; Camilo et al. 2000), which exhibited magnetar-like X-ray outbursts in 2006 and 2016, respectively (Gavriil et al. 2008; Archibald et al. 2016). Before and after its outburst, the radio emission of PSR J1119 − 6127 was as steady as in other radio pulsars. During the outburst, however, the radio emission became variable (Dai et al. 2018). For PSR J1846 − 0258, no radio emission was detected before, during, or after the outburst (e.g. Gotthelf et al. 2000; Archibald et al. 2008).

Radio magnetars are quite different from radio pulsars. The radio spectra of magnetars are flatter than those of radio pulsars. In contrast to the high numbers of radio pulsars, only five magnetars have pulsed radio emission. Studying radio magnetars can therefore shed light on the multiwavelength emission mechanisms of these mysterious compact objects. In this paper, we examine the high-frequency radio observations of two magnetars and compare them with their X-ray light curves to investigate their radio spectral behaviours.

2 OBSERVATIONS AND DATA REDUCTION

2.1 Australia Telescope Compact Array

We observed the two target magnetars with the Australia Telescope Compact Array (ATCA), which consists of six 22-m antennas, with the longest baseline equal to 6 km. The observations were made in the 3mm and 7mm bands for 1E 1547.0 − 5408 on 2017 August 22 with the array configuration EW352. For PSR J1622 − 4950, we observed in the 7mm, 15mm, 4cm and 16cm bands on 2017 June 24 with the array configuration H214. Mars and PKS 1934 − 638 were observed as flux calibrators for the 3mm band and all other bands, respectively. Observation details are given in Table 1.

Table 1. Details of the ATCA and ALMA observations.

Telescope array	Band	Frequency (GHz)	Date in 2017	Observing time (min)	Flux calibrator
ATCA	16cm	2.1	Jun 24	15	PKS 1934 − 638
	4cm	5.5, 9.0	Jun 24	15	PKS 1934 − 638
	15mm	16.7, 21.2	Jun 24	40	PKS 1934 − 638
	7mm	43.0, 45.0	Jun 24	50	PKS 1934 − 638
			Aug 22	100	PKS 1934 − 638
	3mm	93.0, 95.0	Aug 22	120	Mars
ALMA	3	97.5	May 19	8.6	J1617 − 5848
			Sep 15	8.8	J1617 − 5848
	6	233	May 19	18.6	J1617 − 5848

Data reduction was carried out with MIRIAD (Sault, Teuben & Wright 1995)[2] using standard techniques described in the ATCA Users Guide.[3] After applying bandpass, gain and flux calibrations, the task `mfclean` was used to clean the entire primary beam, and then the flux densities were obtained with the task `imfit`. The noise levels of all frequency-band observations are smaller than 0.3 mJy beam^{-1}, and the beam sizes are around 4 arcsec.

2.2 Atacama Large Millimeter/submillimeter Array

We observed PSR J1622 − 4950 with the Atacama Large Millimeter/submillimeter Array (ALMA) in Band 3 (97.5 GHz) and Band 6 (233 GHz) on 2017 May 19 and September 15. Both bands have a usable bandwidth of 7.5 GHz. We also observed J1617 − 5848 as the bandpass and flux calibrators and J1603 − 4904 as the phase calibrator.

For the May observation, 43 12-m antennas were used with baselines from 15.1 m to 1.1 km. Band 3 and Band 6 observations had on-source times of 8.6 and 18.6 min, respectively. For the September observation, 39 12-m antennas were used with baselines from 41.4 m to 9.5 km. The Band 3 observation had an on-source time of 8.8 min, but the Band 6 data were not usable because of poor weather conditions. Details of the observations are listed in Table 1.

We applied the standard data reduction pipeline with CASA v4.7.2 to process the data. We first flagged bad data points, and then applied bandpass, gain and flux calibrations. Finally, total-intensity images were constructed and cleaned using the task `tclean`. The Band 3 image taken in May has a beam size of 1.1 arcsec and an rms noise of 24 μJy beam^{-1}. The September one has a beam size of 0.16 arcsec and a noise of 31 μJy beam^{-1}. The Band 6 image from May has a beam size of 0.45 arcsec and an rms noise of 21 μJy beam^{-1}. All the noise levels are consistent with theoretical values.

We did not detect PSR J1622 − 4950 in the May observation, but the source was detected in September in Band 3, with a flux density of 190 ± 30 μJy.

[2]See https://www.atnf.csiro.au/computing/software/miriad/.
[3]ATCA User Guide https://www.narrabri.atnf.csiro.au/observing/users_guide/html/atug.html.

Table 2. Results of observations on magnetars.

Magnetar	Date in 2017	Frequency (GHz)	Bandwidth (GHz)	Flux density* (mJy)
1E 1547.0 − 5408	Aug 22	43.0	1.84	6.2 ± 0.8
		45.0	1.84	6.3 ± 0.8
		93.0	1.84	8.1 ± 0.9
		95.0	1.84	9.0 ± 1.2
PSR J1622 − 4950	Jun 24	2.1	1.84	< 18
		5.5	1.84	10.8 ± 0.4
		9.0	1.84	3.5 ± 0.1
		16.7	1.84	3.5 ± 0.1
		21.2	1.84	1.43 ± 0.05
		43.0	1.84	0.43 ± 0.03
		45.0	1.84	0.48 ± 0.03
	May 19	97.5	7.5	< 0.072
		233	7.5	< 0.063
	Sep 15	97.5	7.5	0.19 ± 0.03

Note. *The upper limit in flux density is the 3σ detection limit.

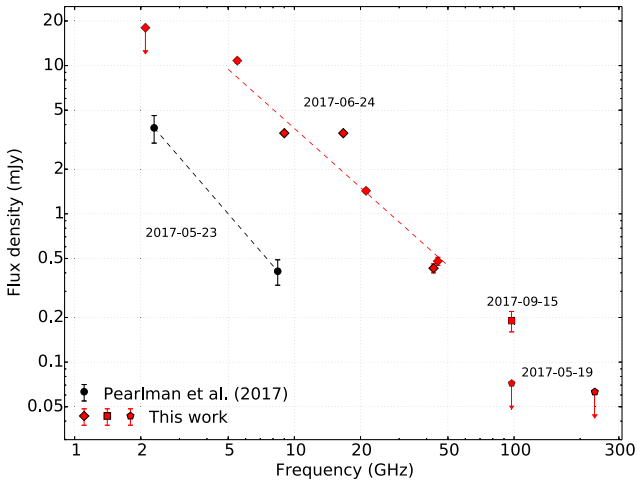

Figure 1. Radio spectra of PSR J1622 − 4950. The black circles are spectra observed by Pearlman et al. (2017). The red diamonds are our ATCA measurements, and red squares and pentagons are our ALMA measurements. The power-law fitting result in 5.5–45 GHz is shown by the red dashed line and yields a spectral index of −1.3 ± 0.2. For some of the data, the error bars are invisible because the errors are smaller than the size of the symbols.

3 RESULTS

3.1 PSR J1622 − 4950

The results of ALMA and ATCA observations of PSR J1622 − 4950 are listed in Table 2 and plotted in Fig. 1. The radio emission was clearly detected from 5.5 to 45 GHz by ATCA. We therefore fitted the steep radio spectrum between 5.5 and 45 GHz with a power law and derived a spectral index of −1.3 ± 0.2. Our ALMA observations at 97.5 and 233 GHz showed non-detection with a 3σ upper limit of 0.08 mJy on May 19. However, the flux density at 97.5 GHz increased to 0.19 mJy after 4 months.

The black points in Fig. 1 are taken from Pearlman et al. (2017). Their observations on 2017 May 23 yield a flux density of 3.8/0.41 mJy at 2.3/8.4 GHz, respectively. Our observations taken one month later, on June 24, however, show flux densities of 10.8 and 3.5 mJy at 5.5 and 9.0 GHz, respectively. The cm-band flux density increased by nearly an order of magnitude in only one month. Our ALMA observations in Band 3 also show an increase in flux density (see Section 4.1 for discussion).

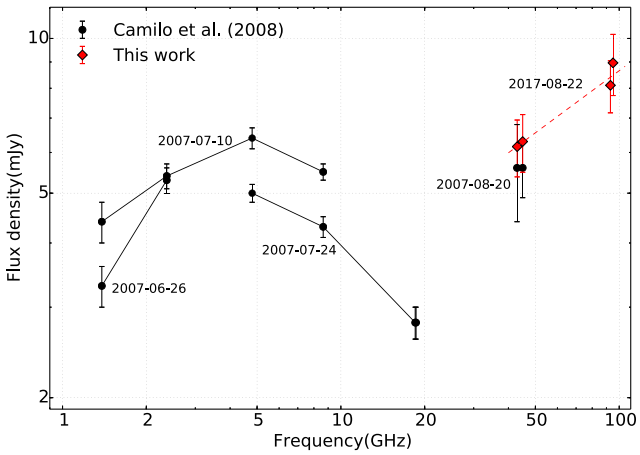

Figure 2. Radio spectra of 1E 1547.0 − 5408. The black circles connected by lines show the data on a different day, taken from Camilo et al. (2008). The red diamonds are our ATCA observation results fitted with a power law, shown as a dashed line. Our results show an inverted spectrum from 43 to 95 GHz with a spectral index of 0.4 ± 0.1.

3.2 1E 1547.0 − 5408

Our ATCA measurements of 1E 1547.0 − 5408 yield flux densities of 6.2 mJy at 43 GHz, 6.3 mJy at 45 GHz, 8.1 mJy at 93 GHz and 9.0 mJy at 95 GHz. The results are listed in Table 2 and plotted in Fig. 2. The spectrum is fitted with a power law, and we found a positive spectral index of 0.4 ± 0.1. The inverted spectrum from 43 to 95 GHz is different from the flat spectrum in the cm band, indicating a possible spectral peak at high frequency (see Section 4.2 for discussion).

The long-term X-ray light curve of 1E 1547.0 − 5408 shows that the absorbed X-ray flux has gradually decreased since the 2009 outburst, but the flux level in 2017 remained much higher than the lowest flux level in 2006 (fig. 3 in Coti Zelati et al. 2020). The X-ray flux during our ATCA observations in 2017 was higher than the X-ray flux in mid-2007, the epoch of radio observations taken by Camilo et al. (2008).

4 DISCUSSION

4.1 Flux evolution

The radio emission of magnetars is known to be variable (e.g. Camilo et al. 2006; Levin et al. 2010), and it has a different evolution from the X-ray emission (Lynch et al. 2015; Pennucci et al. 2015). We obtained radio and X-ray data from the literature and found that the radio emission has a longer rise time than the X-ray emission. The most obvious evidence is the 2013 outburst of SGR J1745 − 2900.

The X-ray and the X-band (8.1–9.3 GHz) radio light curves of SGR J1745 − 2900 taken from the literature are shown in Fig. 3. The radio emission started to decrease about ∼ 400 d after the outburst, giving a radio rise time of 400 d. In contrast, the X-ray outburst is an event of sudden increase in the persistent X-ray flux and it decayed rapidly after the first day. The rise time of radio emission from SGR J1745 − 2900 is thus much longer than that of X-ray emission.

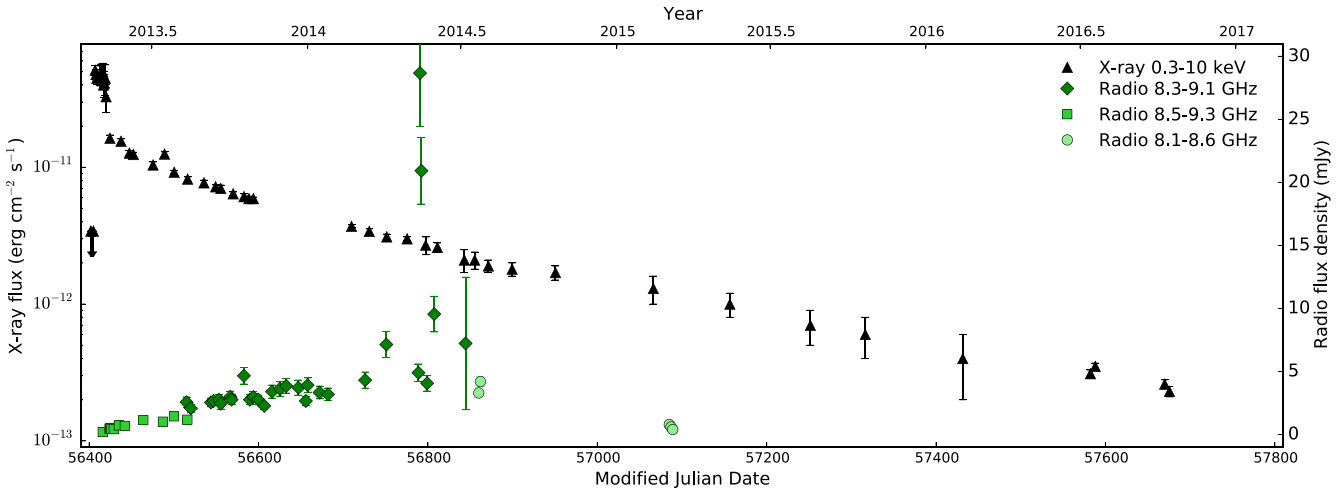

Figure 3. X-ray and radio light curves of SGR J1745 − 2900. The black triangles are absorbed 0.3–10-keV X-ray flux taken from Kennea et al. (2013) and Coti Zelati et al. (2015, 2017). The green diamonds, squares and circles are the X-band radio flux density taken from Lynch et al. (2015), Pennucci et al. (2015) and Torne et al. (2015, 2017). For some of the data, the error bars are invisible because the errors are smaller than the size of symbols.

As described in Section 3.1, the radio flux density of PSR J1622 − 4950 showed a very significant increase while the X-ray flux was decaying in the 2017 outburst; that is, the rise time is different in the radio and the X-ray. The radio emission had a longer rise time than the X-ray emission in the 2017 outburst of PSR J1622 − 4950. Fig. 4 shows the 0.3–10-keV X-ray light curve and the 1.4- and 3.0-GHz radio light curves of PSR J1622 − 4950. According to the X-ray and radio observations, there should be an outburst event between 2006 September and 2007 April (Anderson et al. 2012). The 1.4- and 3.0-GHz observations during this outburst showed very strong variability. Although the trend of radio emission was monotonic decreasing and then went down to undetectable levels in 2015, because there are no data from 2007 to 2009 we cannot rule out that the radio emission was rising during this time.

Moreover, the newly discovered magnetar, Swift J1818.0 − 1607, showed a significant rising trend in radio emission during its 2020 March outburst. The S-band (2.0–2.3 GHz) and the X-band (8.3–8.8 GHz) radio flux densities increased from 0.05 to 0.7 mJy in three epochs from March to July (Maan & van Leeuwen 2020; Majid et al. 2020a, b) and from 0.026 to 1.29 mJy in four epochs from March to August (Majid et al. 2020a, b; Pearlman et al. 2020; Ding et al. 2020), respectively. The increasing trend of radio flux density suggests that the radio rise time is $\gtrsim$ 150 d, which is much longer than the X-ray rise time in outburst (Hu et al. 2020).

For 1E 1547.0 − 5408, there are only a few radio flux density measurements, so we only discuss the 2007 observations performed by Camilo et al. (2008). From Fig. 2, we can see that the flux density increased from June 26 to July 10 at 1.4 GHz and then showed a decreasing trend for 4.8–8.6 GHz two weeks later in July 24. The spectral evolution here gives us another example of the cm-band spectrum seeming to have a longer rise time than the X-ray spectrum during an outburst. However, the increase of the flux density can also be explained by the variability, as the radio emission of magnetars is highly variable.

Furthermore, during the 2003 outburst of XTE J1810 − 197, the X-ray flux evolved as that of a typical magnetar X-ray outburst, with a rapid increase in flux followed by a different scale of decay (Alford & Halpern 2016). The radio flux densities measured in 2003, 2004 and early 2006 were all lower than the measurements in mid-2006 (Halpern et al. 2005; Camilo et al. 2006, 2016), indicating that there could be a very long radio rise period between 2004 and 2006. However, during the 2018 X-ray outburst (Gotthelf et al. 2019), the radio light curve showed no significant increase (Levin et al. 2019). The rise time of the radio emission was thus less than 22 d since outburst, which is much shorter than in other cases.

Rea et al. (2012) pointed out that the emergence of radio emission from magnetars has a delay after the X-ray outburst. This could be attributable to the twisted magnetosphere. The twist and the magnetospheric charge are so strong when the X-ray flux reaches the peak (Thompson, Lyutikov & Kulkarni 2002) that the particle cascades, which emit radio emission, cannot easily propagate outwards. However, the 2013 outburst of SGR J1745 − 2900 showed that radio emission can be seen at the very beginning (Pennucci et al. 2015). The delay of the radio emission can then be better described as a slow rise in radio emission. During the X-ray flux decay, the magnetosphere gradually untwists so that particles have a higher chance of propagating outside the magnetosphere. Hence, the radio emission gradually increases, showing a longer rise time-scale than the X-ray flux.

In addition to radio magnetars, a radio pulsar with magnetar-like bursts, PSR J1119 − 6127, also showed a difference between the evolutions of the X-ray and the radio fluxes. PSR J1119 − 6127 had an X-ray outburst on 2016 July 26. The radio flux density of PSR J1119 − 6127 was steady at $\sim$ 1 mJy at 1.4 GHz before this 2016 outburst. However, the radio emission became variable after the outburst. Observations showed that the radio emission disappeared after July 29 (Burgay et al. 2016a). On August 9, the radio emission was reactivated, but the flux density was significantly weaker than the pre-outburst value (Burgay et al. 2016b). After the reactivation, the radio flux density gradually increased to its highest value of $\sim$ 5.6 mJy on August 31, one month after the X-ray outburst (fig. 1 in Dai et al. 2018). The radio flux density then decreased to the minimum value of $\sim$ 0.14 mJy and then recovered to the previous steady flux density of 1 mJy. The variable radio emission took one month to reach its highest value during an X-ray outburst. This longer rise time is similar to that for other radio magnetars. The variable state of radio emission caused by the X-ray outburst can thus be described by a magnetar model. In normal rotation-powered radio

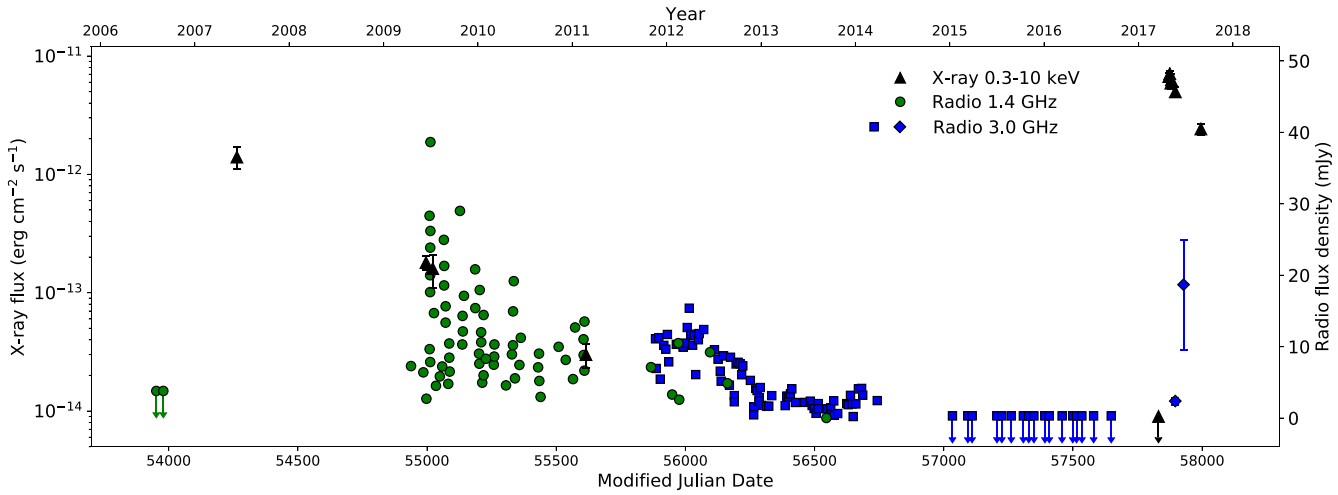

Figure 4. X-ray and radio light curves of PSR J1622 − 4950. The black triangles are absorbed 0.3–10 keV X-ray flux taken from Anderson et al. (2012) and Camilo et al. (2018). The green circles and the blue squares are respectively the 1.4- and 3-GHz radio flux density taken from Scholz et al. (2017). The blue diamonds are the 3-GHz radio flux density derived from Pearlman et al. (2017) and this work (Fig. 1) based on the observed spectral indices. For some of the data, the error bars are invisible because the errors are smaller than the size of symbols.

pulsars, the radio emission is believed to be generated by particles in open magnetic field lines near the polar region. Before and after the X-ray outburst, PSR J1119 − 6127 reacted as a rotation-powered pulsar. The radio emission came from the radio beam steadily. At the time of the X-ray outburst, the activity of the neutron star made the magnetosphere twisted so that the original open field lines became unstable (Beloborodov 2009; Braithwaite & Spruit 2004). Hence, the radio emission from the radio beam disappeared. Similarly, the magnetosphere of PSR J1622 − 6127 changed to a magnetar-like structure. The radio emission gradually increased as a result of the untwisting of the magnetosphere. At the end of the outburst, the magnetosphere gradually re-configured itself back to the structure of a normal rotation-powered radio pulsar so that the radio emission became stable again. The difference between the radio pulse profiles for the radio steady state and the variable state (Archibald et al. 2017; Majid et al. 2017; Dai et al. 2018) can also support the transition between the usual radio pulsar model and a radio magnetar model.

All five radio magnetars and one magnetar-like rotation-powered pulsar show hints of a rise-time difference between the X-ray and radio emission. Although not all the outbursts show similar phenomena, the evolution difference can provide further insight into the relationship between X-ray and radio emission from magnetars during an outburst.

4.2 Double-peak spectra

The observed radio spectra of 1E 1547.0 − 5408 and PSR J1622 − 4950 show a peak at a few GHz (Camilo et al. 2008; Levin et al. 2010; Keith et al. 2011). This spectral feature is the so-called gigahertz-peaked spectrum (GPS), which is used to describe the spectral turn-over near one GHz for some pulsars (Kijak et al. 2011). Detailed spectral analysis shows that both spectra can be fitted with a log-parabola and that the peak is at about 5.0 GHz for 1E 1547.0 − 5408 and 8.3 GHz for PSR J1622 − 4950 (Kijak et al. 2013). The fourth radio magnetar discovered, SGR J1745 − 2900, also shows a GPS with a peak at ∼ 2 GHz (Pennucci et al. 2015). Moreover, simultaneous wide-band observations from 0.7 to 4 GHz for XTE J1810 − 197 show an inverted spectrum (Dai et al. 2019). Compared with its steep cm-band (4.85–14.60 GHz) spectra in previous observations (Lazaridis et al. 2008), XTE J1810 − 197 is likely to have a GPS feature as well, with a peak at ∼ 4 GHz. The reason that pulsars have a GPS is probably the low-frequency absorption from the surrounding environment of pulsars or the molecular clouds in the line of sight (Kijak et al. 2011). Both 1E 1547.0 − 5408 and PSR J1622 − 4950 are in SNRs (Lamb & Markert 1981; Gelfand & Gaensler 2007; Levin et al. 2010; Anderson et al. 2012), and SGR J1745 − 2900 is only 2 arcsec away from the Galactic Centre (Kennea et al. 2013). The X-ray, optical and infrared (IR) images of XTE J1810 − 497 show no evidence of association with another source (Gotthelf et al. 2004). If the 0.7–4 GHz-band spectrum of XTE J1810 − 197 is actually a GPS, the absorption could take place in the molecular clouds along the line of sight, or the reason for the GPS in magnetars could be different from that in radio pulsars.

Moreover, the spectra of radio magnetars could have not only a single peak at GHz but also a second peak at a few hundred GHz. Observations of SGR J1745 − 2900 in 2015 show an inverted spectrum from 2.54 to 291 GHz (Torne et al. 2017). However, not all the data points are well fitted. The cm-band (2.54–8.35 GHz) spectral index is negative, and the flux density probably decreases above 200 GHz. The spectral shape can thus be better described by multiple components. Considering the GPS at lower frequency, the observed spectral shape in 2015 may have double peaks at ∼ 2 and ∼ 200 GHz. Comparing the spectra of SGR J1745 − 2900 at different epochs from 2014 to 2015, the cm-band flux density decreased by about 5 times, while the submm-band flux density increased by about 4 times (Torne et al. 2015, 2017). This evolution difference supports the theory of a double-component radio spectrum.

In addition, the observed inverted spectrum of 1E 1547.0 − 5408 between 43 and 95 GHz gives us a hint of a peak over 100 GHz (Fig. 2). By combining observations in the cm and the mm bands, 1E 1547.0 − 5408 shows a double-peak spectrum similar to that in SGR J1745 − 2900. The nature of the hundred-gigahertz peaked spectra remains unknown. The double peaks in the spectrum are probably the result of two different emission mechanisms in different bands. Radio emission from pulsars is known to be coherent, and is characterized by a high brightness temperature. On the other hand, observations

in the infrared and higher energies show that the pulsar emission is incoherent (e.g. Shklovsky 1970), implying a transition between coherence and incoherence. It has been speculated that the transition should lie in the mm/submm range (Michel 1982). The spectra of both 1E 1547.0 − 5408 and SGR J1745 − 2900 show that the transition between the two peaks is located at ∼ 20–40 GHz, which could mark the end of coherent emission and the start of incoherent emission. There is only one example of a double-peak spectra from SGR J1745 − 2900 and one candidate from 1E 1547.0 − 5408. More high-frequency radio observations are needed to discuss and verify the double-peak spectra.

However, our ALMA observations of PSR J1622 − 4950 do not indicate any peak feature at a few hundred GHz. The high-frequency 88.5-GHz observations of XTE J1810 − 197 in 2006 and 2007 also show no hint of a hundred-gigahertz-peaked feature (Camilo et al. 2007b). Because the hundred-gigahertz peak of SGR J1745 − 2900 in 2014 was ∼ 4 times weaker than in 2015 (Torne et al. 2015, 2017), there is still the possibility that the high-frequency component of PSR J1622 − 4950 and XTE J1810 − 197 was not dominant at the time of their observations.

4.3 The turning off of radio emission

All previously observed radio emission from magnetars can be associated with an X-ray outburst, except for the archival radio data of PSR J1622 − 4950 before 2003 obtained by Levin et al. (2010) because of the lack of X-ray data. The radio emission from XTE J1810 − 197 and PSR J1622 − 4950 disappeared years after an X-ray outburst (Camilo et al. 2016; Scholz et al. 2017). Although the last X-ray outburst of 1E 1547.0 − 5408 was in 2009, 8.5 yr before our radio observations, we still had detection in the mm band. There are three possible explanations. The first is that once the radio emission is turned on, it needs to be turned off by other activities. We consider this less likely, because there was no evidence of unusual changes in properties such as the spin frequency or X-ray pulse profile when the radio emission was undetectable (Camilo et al. 2016; Scholz et al. 2017). Another possibility is simply that the 2009 X-ray outburst has not ended, so that the X-ray-outburst-associated radio emission continued. The final one is that the radio emission is not associated with the X-ray outburst but with the X-ray flux level. The X-ray flux level in 2017 was higher than that in 2007, when the radio emission of 1E 1547.0 − 5408 was discovered (Coti Zelati et al. 2020), so we can still detect radio emission. Once the X-ray flux decreases to a certain level, the radio emission may disappear. The study by Camilo et al. (2016) of XTE J1810 − 197 also suggests that the radio disappearance is most likely due to the decrease of X-ray flux; however, these authors emphasize that the X-ray flux change is only 20 per cent. More observations in the X-ray and radio and more timing and/or spectral analysis are needed to confirm the radio turn-off criteria.

5 SUMMARY

We performed an analysis of the radio observations of two magnetars, 1E 1547.0 − 5408 and PSR J1622 − 4950. The former showed an inverted spectrum from 43 to 95 GHz, indicating a peak at high frequency. The broad-band radio spectra of 1E 1547.0 − 5408 is similar to that of SGR J1745 – 2900. Both of them may have different emission mechanisms in the cm and submm bands, resulting in double-peak spectra with peaks at a few GHz and a few hundred GHz. Our observations of PSR J1622 − 4950 revealed a steep spectrum from 5.5 to 45 GHz. By comparing observations in different epochs, we found that PSR J1622 − 4950 exhibited a significant increase in radio flux density while the X-ray flux was decreasing. We further obtained X-ray and radio data of radio magnetars and a magnetar-like radio pulsar from the literature and found, for the first time, that the rise time of radio emission is much longer than that of X-ray emission in some magnetar outbursts. More simultaneous broad-band observations in different epochs are needed to confirm these properties and to study the origin of radio emission from magnetars.

ACKNOWLEDGEMENTS

The Australia Telescope Compact Array is part of the Australia Telescope National Facility, which is funded by the Australian Government for operation as a National Facility managed by CSIRO. This paper makes use of the following ALMA data: ADS/JAO.ALMA#2016.1.00456.T. ALMA is a partnership of the ESO (representing its member states), NSF (USA) and NINS (Japan), together with the NRC (Canada), MOST and ASIAA (Taiwan) and KASI (Republic of Korea), in cooperation with the Republic of Chile. The Joint ALMA Observatory is operated by the ESO, AUI/NRAO and NAOJ. C.-Y. Chu and H.-K. Chang are supported by the Ministry of Science and Technology (MOST) of the Republic of China (Taiwan) under the grant MOST 108-2112-M-007-003. C.-Y. Ng is supported by a GRF grant from the Hong Kong Government under HKU 17300215P. A. K. H. Kong is supported by the Ministry of Science and Technology (MOST) of Republic of China (Taiwan) under the grants MOST 105-2119-M-007-028-MY3 and 108-2628-M-007-005-RSP.

Note: After our manuscript was submitted, Torne et al. (2020) published the spectrum results of XTE J1810 − 197 which may show a sign of hundred-gigahertz peaked spectra.

DATA AVAILABILITY

The data underlying this article are available in the article. ATCA data are available through the Australia Telescope Online Archive.[4] ALMA data are available through the ALMA Science Archive.[5]

REFERENCES

Alford J. A. J., Halpern J. P., 2016, ApJ, 818, 122
Anderson G. E. et al., 2012, ApJ, 751, 53
Archibald A. M., Kaspi V. M., Livingstone M. A., McLaughlin M. A., 2008, ApJ, 688, 550
Archibald R. F., Kaspi V. M., Tendulkar S. P., Scholz P., 2016, ApJ, 829, L21
Archibald R. F. et al., 2017, ApJ, 849, L20
Beloborodov A. M., 2009, ApJ, 703, 1044
Bochenek C. D., Ravi V., Belov K. V., Hallinan G., Kocz J., Kulkarni S. R., McKenna D. L., 2020, Nature, 587, 59
Braithwaite J., Spruit H. C., 2004, Nature, 431, 819
Burgay M., Possenti A., Kerr M., Esposito P., Rea N., Zelati F. C., Israel G. L., Johnston S., 2016a, Astron. Telegram, 9286, 1
Burgay M., Possenti A., Kerr M., Esposito P., Rea N., Zelati F. C., Israel G. L., Johnston S., 2016b, Astron. Telegram, 9366, 1
Burgay M. et al., 2020, Astron. Telegram, 13783, 1
Camilo F., Kaspi V. M., Lyne A. G., Manchester R. N., Bell J. F., D'Amico N., McKay N. P. F., Crawford F., 2000, ApJ, 541, 367
Camilo F., Ransom S. M., Halpern J. P., Reynolds J., 2007a, ApJ, 666, L93

[4] https://atoa.atnf.csiro.au/
[5] https://almascience.eso.org/asax/

Camilo F., Ransom S. M., Halpern J. P., Reynolds J., Helfand D. J., Zimmerman N., Sarkissian J., 2006, Nature, 442, 892
Camilo F., Reynolds J., Johnston S., Halpern J. P., Ransom S. M., 2008, ApJ, 679, 681
Camilo F. et al., 2007b, ApJ, 669, 561
Camilo F. et al., 2016, ApJ, 820, 110
Camilo F. et al., 2018, ApJ, 856, 180
Coti Zelati F. et al., 2015, MNRAS, 449, 2685
Coti Zelati F. et al., 2017, MNRAS, 471, 1819
Coti Zelati F. et al., 2020, A&A, 633, A31
Dai S. et al., 2018, MNRAS, 480, 3584
Dai S. et al., 2019, ApJ, 874, L14
Ding H., Deller A. T., Lower M. E., Shannon R. M., 2020, Astron. Telegram, 14005, 1
Duncan R. C., Thompson C., 1992, ApJ, 392, L9
Eatough R. P. et al., 2013, Nature, 501, 391
Enoto T. et al., 2020, Astron. Telegram, 13551, 1
Esposito P. et al., 2020, ApJ, 896, L30
Evans P. A. et al., 2020, GRB Coordinates Network, 27373, 1
Gavriil F. P., Gonzalez M. E., Gotthelf E. V., Kaspi V. M., Livingstone M. A., Woods P. M., 2008, Science, 319, 1802
Gelfand J. D., Gaensler B. M., 2007, ApJ, 667, 1111
Gotthelf E. V., Halpern J. P., Buxton M., Bailyn C., 2004, ApJ, 605, 368
Gotthelf E. V., Vasisht G., Boylan-Kolchin M., Torii K., 2000, ApJ, 542, L37
Gotthelf E. V. et al., 2019, ApJ, 874, L25
Halpern J. P., Gotthelf E. V., Becker R. H., Helfand D. J., White R. L., 2005, ApJ, 632, L29
Halpern J. P., Gotthelf E. V., Reynolds J., Ransom S. M., Camilo F., 2008, ApJ, 676, 1178
Hu C.-P. et al., 2020, ApJ, 902, 1
Ibrahim A. I. et al., 2004, ApJ, 609, L21
Israel G. L., Rea N., Zelati F. C., Esposito P., Burgay M., Mereghetti S., Possenti A., Tiengo A., 2014, Astron. Telegram, 6370, 1
Israel G. L. et al., 2010, MNRAS, 408, 1387
Kaneko Y. et al., 2010, ApJ, 710, 1335
Karuppusamy R. et al., 2020, Astron. Telegram, 13553, 1
Keith M. J., Johnston S., Levin L., Bailes M., 2011, MNRAS, 416, 346
Kennea J. A. et al., 2013, ApJ, 770, L24
Kijak J., Lewandowski W., Maron O., Gupta Y., Jessner A., 2011, A&A, 531, A16
Kijak J., Tarczewski L., Lewandowski W., Melikidze G., 2013, ApJ, 772, 29
Kuiper L., Hermsen W., den Hartog P. R., Urama J. O., 2012, ApJ, 748, 133
Lamb R. C., Markert T. H., 1981, ApJ, 244, 94
Lazaridis K., Jessner A., Kramer M., Stappers B. W., Lyne A. G., Jordan C. A., Serylak M., Zensus J. A., 2008, MNRAS, 390, 839
Levin L. et al., 2010, ApJ, 721, L33
Levin L. et al., 2019, MNRAS, 488, 5251
Lynch R. S., Archibald R. F., Kaspi V. M., Scholz P., 2015, ApJ, 806, 266
Maan Y., van Leeuwen J., 2020, Astron. Telegram, 13560, 1
Majid W. A., Pearlman A. B., Dobreva T., Horiuchi S., Kocz J., Lippuner J., Prince T. A., 2017, ApJ, 834, L2
Majid W. A., Pearlman A. B., Prince T. A., Naudet C. J., Bansal K., 2020b, Astron. Telegram, 13898, 1
Majid W. A., Pearlman A. B., Prince T. A., Naudet C. J., Kocz J., Horiuchi S., Enoto T., Younes G., 2020a, Astron. Telegram, 13649, 1
Mereghetti S. et al., 2009, ApJ, 696, L74
Michel F. C., 1982, Rev. Mod. Phys., 54, 1
Mori K. et al., 2013, ApJ, 770, L23
Ng C. Y. et al., 2011, ApJ, 729, 131
Olausen S. A., Kaspi V. M., 2014, ApJS, 212, 6
Palmer D. M., 2020, Astron. Telegram, 13675, 1
Pearlman A. B., Majid W. A., Prince T. A., Horiuchi S., Kocz J., Lazio T. J. W., Naudet C. J., 2017, Astron. Telegram, 10581, 1
Pearlman A. B., Majid W. A., Prince T. A., Naudet C. J., Bansal K., Horiuchi S., 2020, Astron. Telegram, 13966, 1
Pennucci T. T. et al., 2015, ApJ, 808, 81
Rea N., Pons J. A., Torres D. F., Turolla R., 2012, ApJ, 748, L12
Sault R. J., Teuben P. J., Wright M. C. H., 1995, in Shaw R. A., Payne H. E., Hayes J. J. E., eds, ASP Conf. Ser. Vol. 77, Astronomical Data Analysis Software and Systems IV. Astron. Soc. Pac., San Francisco, p. 433
Savchenko V., Neronov A., Beckmann V., Produit N., Walter R., 2010, A&A, 510, A77
Scholz P., Kaspi V. M., 2011, ApJ, 739, 94
Scholz P. et al., 2017, ApJ, 841, 126
Shannon R. M., Johnston S., 2013, MNRAS, 435, L29
Shklovsky I. S., 1970, ApJ, 159, L77
The CHIME/FRB Collaboration et al., 2020, Nature, 587, 54
Thompson C., 2008, ApJ, 688, 499
Thompson C., Lyutikov M., Kulkarni S. R., 2002, ApJ, 574, 332
Torne P. et al., 2015, MNRAS, 451, L50
Torne P. et al., 2017, MNRAS, 465, 242
Torne P. et al., 2020, A&A, 640, L2
von Kienlin A. et al., 2012, ApJ, 755, 150
Woods P. M. et al., 2004, ApJ, 605, 378
Zhu W. et al., 2020, Astron. Telegram, 14084, 1

This paper has been typeset from a TEX/LATEX file prepared by the author.